

Article

# Calibration Factor for ASCE 41-17 Modeling Parameters for Stocky Rectangular RC Columns

Sang Whan Han <sup>1</sup>, Chang Seok Lee <sup>1,\*</sup>, Mary Ann Paz Zambrana <sup>1</sup> and Kihak Lee <sup>2</sup>

<sup>1</sup> Department of Architectural Engineering, Hanyang University, Seoul 04763, Korea; swhan82@gmail.com (S.W.H.); arq.ann.paz@gmail.com (M.A.P.Z.)

<sup>2</sup> Department of Architectural Engineering, Sejong University, Seoul 05006, Korea; kihaklee@sejong.ac.kr

\* Correspondence: mtsonicc@gmail.com; Tel.: +82-2-2220-0566

Received: 15 October 2019; Accepted: 26 November 2019; Published: 29 November 2019



**Featured Application:** Calibration factor for ASCE 41-17 modeling parameters of stocky columns.

**Abstract:** Existing old reinforced concrete (RC) buildings could be vulnerable to large earthquake events. Most columns in such buildings have insufficient reinforcement details, which may experience failure during an early loading stage. The failure of columns may lead to partial or complete collapse of entire building systems. To prepare for an adequate retrofit plan for columns, it is necessary to simulate the cyclic behavior of columns using a numerical model with adequate values of constituent modeling parameters. The nonlinear component modeling parameters are specified in ASCE 41-17. However, the experiments on stocky RC columns suggest that ASCE 41-17 nonlinear component modeling parameters do not reflect the RC column behavior adequately. To accurately simulate the nonlinear load–deformation responses of stocky RC columns with low span-to-depth ratio, this study proposes a calibration factor for ASCE 41-17 RC column modeling parameters. For this purpose, this study collected test data of 47 stocky column specimens. Based on the test data, empirical equations including the calibration factor for modeling parameters “*a*” and “*b*” in ASCE 41-17 were proposed. The accuracy of the proposed equation was verified by comparing the measured and calculated envelope curves.

**Keywords:** columns; cyclic behavior; low height-to-depth ratio; modeling parameters; calibration

## 1. Introduction

Reinforced concrete (RC) buildings not designed according to modern seismic design codes can be vulnerable to collapse during earthquakes [1]. Postearthquake researches indicated that columns are one of the most critical structural components in seismically active regions due to their nonductile reinforcement details [2–6]. Deficiencies such as lack of confinement due to widely spaced transverse reinforcement [1], ineffective anchorage length, and insufficient development length [7–11] can cause premature shear failure in RC columns [12,13], thus leading to rapid lateral strength degradation [14] or even collapse [15–18]. To understand the seismic behavior of such columns under earthquakes and to propose an adequate retrofit scheme, the seismic capacity of RC columns with nonseismic reinforcement details should be estimated.

To predict the seismic capacity of such RC columns with acceptable accuracy, an accurate backbone curve is required, which defines the lateral load–deformation capacity of a structural component. An extensive amount of research has been carried out on developing backbone curves of RC columns [14,15,19–22]. The nonlinear load–deformation relation proposed by ASCE 41-17 [23] (as noted hereafter as ASCE 41-17) is most widely used in the fields. This standard is provided to

conduct seismic evaluation and retrofit of existing building by the American Society of Civil Engineer (ASCE), which includes performance objectives and seismic hazards, Tiers 1–3 seismic performance evaluation procedures, and retrofit.

Due to the importance of this standard, it has been continuously revised since its first release to provide a better accuracy in estimating nonlinear load–deformation response of structural components.

Ghannoum and Matamoros [24] proposed equations for RC columns to calculate modeling parameters to construct a backbone curve, instead of using fixed values used in the previous standard [25]. These equations are shown in ASCE 41-17, which lead to better estimation of modeling parameters compared with those in the previous standard. Accurate estimation of modeling parameters is a key factor in seismic performance evaluation [26] by selecting input seismic ground motions [27].

However, the deformation parameters suggested in ASCE 41-17 do not consider height-to-depth ratios, which can significantly alter the column behavior [19,28]. For RC members with a height-to-depth ratio lower than 2 (as noted hereafter as stocky columns), their cyclic behavior is always dominated by shear [5,29,30]. Therefore, shear deformation induced by shear cracking expansion can be significant [31,32]. When the ASCE 41-17 modeling parameter equations are applied to columns with low height-to-depth ratios (stocky columns), the estimation error between measured and estimated values may become significant.

In order to better estimate the load–deformation response of stocky RC columns, this study proposes a calibration factor for the equations of deformation modeling parameters provided in ASCE 41-17. For this purpose, the values of deformation parameters for 47 rectangular RC columns with low height-to-depth ratios are extracted. To minimize the difference between measured values and those predicted by the ASCE 41-17 equations, the calibration factor was estimated for individual column specimens. Then, the empirical equations including the calibration factor are proposed from regression analyses.

## 2. Backbone Curve for RC Columns in ASCE 41-17

In ASCE 41-17, an idealized nonlinear load–deformation relation for a structural component is provided to represent a generalized backbone curve, as shown in Figure 1. In Figure 1,  $V$  and  $V_y$  are the column shear force and the column yield shear strength, respectively, and  $\theta$  is the drift ratio;  $a$  and  $b$  are the parameters representing plastic drift ratios, for cases when a strength degradation begins and the shear force drops to the point “D”, respectively.

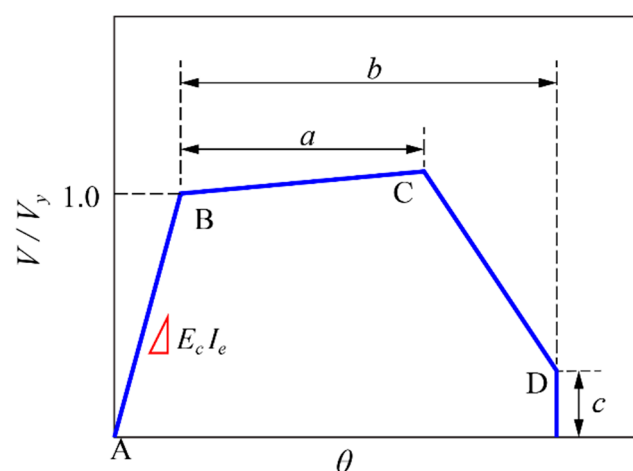


Figure 1. Generalized load–deformation relation.

The generalized load–deformation relation consists of a linear portion and a nonlinear portion. The linear portion corresponds to the segment between points A and B, which can be determined using the effective stiffness of a structural component. In ASCE 41-17, equations are given to calculate

the effective stiffness for various structural components. For RC columns, the proposed equations to calculate the effective stiffness are summarized in Table 1, where  $E_c$  is the modulus of elasticity of concrete,  $I_g$  is the moment of inertia of the concrete gross section,  $A_w$  is the summation of the net horizontal cross-sectional area for concrete in the direction of loading, and  $A_g$  is the gross sectional area of the column.

**Table 1.** Effective stiffness equations proposed by ASCE 41-17.

Component	Flexural Rigidity	Shear Rigidity	Axial Rigidity
Columns with compression caused by design gravity loads	$0.7E_cEI_g$	$0.4E_cEA_w$	$E_cEA_g$
Columns with compression caused by design gravity loads or with tension	$0.3E_cEI_g$	$0.4E_cEA_w$	$0.4E_cEA_g$

The nonlinear portion is governed by two deformation parameters, that is, modeling parameters  $a$  and  $b$ . For rectangular RC columns, parameter  $a$  can be calculated using Equation (1):

$$a_{ASCE} = 0.042 - 0.043 \frac{P}{A_g f_c} + 0.63 \rho_t - 0.023 \frac{V_y}{V_0} \geq 0, \tag{1}$$

where  $P$  is the axial compressive load applied on the column section,  $f_c$  is the concrete compressive strength,  $\rho_t$  is the ratio of the area of distributed transverse reinforcement to the concrete gross area perpendicular to that reinforcement, and  $V_y$  is the yield shear strength of the column. The column shear strength  $V_0$  is calculated from Equation (2) provided in ASCE 41-17 for RC columns:

$$V_0 = \left[ \frac{A_v f_{yt} d}{s} + \left( \frac{6 \sqrt{f_c}}{a_v/h} \sqrt{1 + \frac{P}{6 A_g \sqrt{f_c}}} \right) 0.8 A_g \right], \tag{2}$$

where  $a_v/h$  is the height-to-depth ratio of the column;  $k_{nl}$  is 1.0 for a displacement ductility demand ( $\mu$ ) less than or equal to 2 and 0.7 for  $\mu \geq 6$ , where  $\mu$  is calculated as  $\theta/\theta_y$  and  $\theta_y$  is the yield drift ratio as shown in Figure 2. For  $\mu$  between 2 and 6,  $k_{nl}$  is estimated using interpolation.

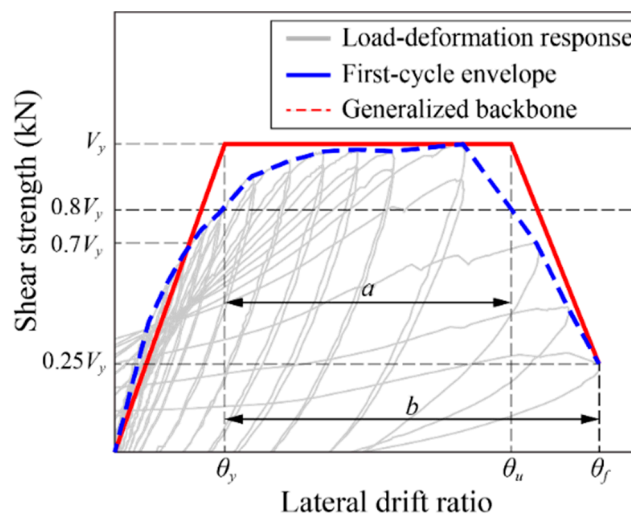


**Figure 2.** Measured modeling parameters from a measured first-cycle envelope.

The load–deformation response representing a reduced resistance is predicted using modeling parameter  $b$ , which is calculated using Equation (3):

$$b_{ASCE} = \frac{0.5}{5 + \frac{P}{0.8A_g f_c} \frac{1}{\rho_t} \frac{f_c}{f_{yt}}} - 0.01 \geq a_{ASCE}, \quad (3)$$

where  $f_{yt}$  is the yield strength of the transverse reinforcement and modeling parameter  $b$  must be greater than or equal to modeling parameter  $a$ .

### 3. Estimating the Values of Modeling Parameters from the Measured Cyclic Curves

The modeling parameters  $a$  and  $b$  were extracted from the first-cyclic envelope curve of RC columns. The first-cycle envelope curve can be constructed by connecting each point of the peak displacements during the first cycle of each increment of loading (or deformation) [23,33]. Figure 2 illustrates the extraction of the modeling parameters  $a$  and  $b$ .

In Figure 2, the values for the maximum shear strength  $V_y$  are identical to the maximum ordinate values of the first-cycle envelope. Yield drift ratio  $\theta_y$  was obtained according to the procedure proposed by Sezen et al. [2]. A secant line is projected from the origin to the intersection point on the first-cycle envelope curve and a horizontal line at  $0.7V_y$ . The secant line was extended, until it reached the horizontal line drawn at  $V_y$ . Then,  $\theta_y$  is the abscissa of the intersection of these two lines.

Drift ratio  $\theta_u$  is a lateral drift ratio, at which a significant (more than or equal to 20%) lateral resistance degradation from  $V_y$  occurs. In ASCE 41-17,  $\theta_f$  is defined as a lateral drift ratio at axial failure. However, due to the scarcity of column specimens tested up to the onset of axial failure [24,34],  $\theta_f$  is defined as a lateral drift ratio, when the lateral strength decreases to 25% of  $V_y$ .

The values of modeling parameters  $a$  and  $b$  can be calculated using Equations (4) and (5), respectively:

$$a = \theta_u - \theta_y, \quad (4)$$

$$b = \theta_f - \theta_y. \quad (5)$$

### 4. Stocky RC Column Database

The PEER Structural Performance Database provides the test data of 246 rectangular RC columns. Among them, only 47 columns have section-to-depth ratios less than or equal to 2.0. Only a limited number of cyclic tests were conducted for stock columns. In this study, 47 rectangular RC column test specimens with height-to-depth ratios ( $a_v/h$ ) less than or equal to 2.0 (stocky columns) were collected from the PEER Structural Performance Database [35]. All the 47 specimens experienced a strength drop by more than 20%.

The ranges of important parameters are summarized below:

Height-to-depth ratio	$1.0 \leq a_v/h \leq 2.0$
Section width (mm)	$160 \leq b \leq 500$
Section height (mm)	$160 \leq h \leq 914$
Center-to-center spacing of a transverse reinforcement (mm)	$20 \leq s \leq 406$
Longitudinal reinforcement ratio (%)	$1.27 \leq \rho_l \leq 6.94$
Transverse reinforcement ratio (%)	$0.08 \leq \rho_t \leq 1.64$
Measured compressive strength of concrete	$14 \leq f_c \leq 118$
Measured yield strength of longitudinal reinforcement	$323 \leq f_{yl} \leq 510$
Measured yield strength of transverse reinforcement	$258 \leq f_{yt} \leq 1424$
Axial load ratio (%)	$0 \leq v \leq 80.1; v = P/(A_g f_c)$

To estimate the error between the measured and calculated values of the modeling parameters, absolute relative errors (AREs) were calculated using Equation (6):

$$ARE = \left| \frac{MP_{meas} - MP_{ASCE}}{MP_{meas}} \right|, \tag{6}$$

where  $MP_{meas}$  is the measured modeling parameter value for  $a$  and  $b$  extracted from the first-cycle envelope curve and  $MP_{ASCE}$  is the parameter value for  $a$  and  $b$  calculated using Equations (1) and (3), respectively.

Figure 3 shows the relationship of the calculated ARE and the shear span-to-section height ratio ( $a_v/h$ ), in which 246 specimens with  $a_v/h$  ranging from 1 to 7.3 were included. The test data for these specimens were also obtained from the PEER Structural Performance Database [35]. The solid and dashed lines in Figure 3 represent the mean ARE values obtained from the moving windows analyses. With an increase in  $a_v/h$ , the mean values of ARE for parameters  $a$  and  $b$  [ $\mu_{ARE(a)}, \mu_{ARE(b)}$ ] generally decrease. In the case of  $a_v/h \geq 2.0$ ,  $\mu_{ARE(a)}$  and  $\mu_{ARE(b)}$  approach approximately 0.5 and 0.3, respectively. However, with the decrease in  $a_v/h$  within the range of  $a_v/h$  less than 2.0,  $\mu_{ARE(a)}$  and  $\mu_{ARE(b)}$  increase sharply, which indicates that the errors associated with the ASCE 41-17 equations for parameters  $a$  and  $b$  become more significant. Thus, it is necessary to propose a calibration factor for Equations (1) and (3) for columns with  $a_v/h \leq 2.0$ .

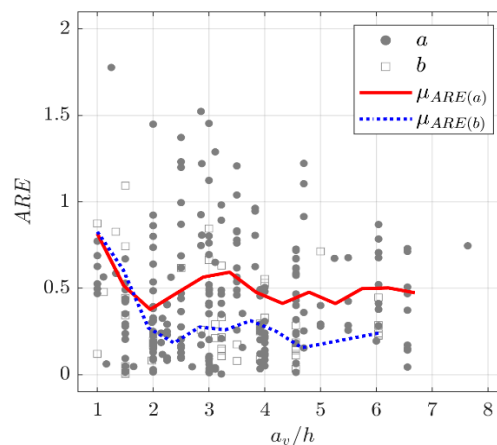


Figure 3. Absolute relative error (ARE) between the measured and ASCE modeling parameters.

### 5. Regression Analysis

The original equations of ASCE 41-17 do not include the influence of a height-to-depth ratio; however, it was revealed in the previous section that there was a considerable amount of error in the modeling parameter predictive equation proposed by ASCE 41-17 when the height-to-depth ratio was lower than 2.0. For this reason, a calibration factor was proposed to minimize error.

Linear regression was used to introduce a calibration factor for the modeling parameter predictive equation of ASCE 41-17 to calculate more accurately the values of parameters  $a$  and  $b$ . The measured modeling parameters extracted from the first-cycle envelope curve is shown in Table 2.

To propose an empirical calibration factor, various candidate predictor variables frequently used in the past research [14,22,52–55] were considered. Considered candidate predictor variables include: longitudinal reinforcement ratio ( $\rho_l$ ), transverse reinforcement ratio ( $\rho_t$ ), axial load ratio ( $v = P/(f'_c A_g)$ ), measured concrete compressive strength ( $f_c$ ), column shear span ( $a_v$ ), height-to-depth ratio ( $a_v/h$ ), ratio of a transverse bar spacing to a column depth ( $s/h$ ), ratio of a strength contribution of longitudinal reinforcements to that of concrete ( $f_{yl} A_{sl} / f'_c A_g$ ), ratio of a strength contribution of concrete axial strength to that of transverse reinforcements ( $f'_c A_g / f_{yt} A_{st}$ ).

**Table 2.** Physical properties and measured deformation parameters of the selected specimens.

No.	ID	$a_v/h$	$b$ (mm)	$h$ (mm)	$s$ (mm)	$\rho_l$ (%)	$\rho_t$ (%)	$f_c$ (MPa)	$f_{yt}$ (MPa)	$a_{meas}$ (%)	$b_{meas}$ (%)	Reference
1	SC9	1.33	457	914	406	1.88	0.08	16	400	0.36	-	[36]
2	CB060C	1.16	278	278	52	2.75	0.78	46	414	0.50	-	[37]
3	H-2-1_3	2.00	200	200	40	2.65	0.71	23	364	1.51	-	[38]
4	H-2-1_5	2.00	200	200	50	2.65	0.57	23	364	1.96	-	
5	HT-2-1_3	2.00	200	200	60	2.65	0.71	20	364	2.03	-	
6	HT-2-1_5	2.00	200	200	75	2.65	0.57	20	364	1.99	-	
7	I18	2.00	500	500	254	2.12	0.20	33	258	1.64	-	[39]
8	I21	2.00	500	500	254	2.12	0.20	32	258	0.98	-	
9	HPRC10-63	1.50	200	200	35	1.27	0.68	22	344	1.33	-	[40]
10	HPRC19-32	1.50	200	200	20	1.27	1.19	21	344	1.15	-	
11	N-18M	1.50	300	300	100	2.68	0.21	27	380	0.62	10.16	[41]
12	N-27C	1.50	300	300	100	2.68	0.21	27	380	0.57	3.00	
13	N-27M	1.50	300	300	100	2.68	0.21	27	380	0.94	4.70	
14	2D16RS	2.00	200	200	50	2.01	0.48	32	316	2.85	-	[42]
15	4D13RS	2.00	200	200	50	2.65	0.48	30	316	1.00	-	
16	CA025C	1.50	200	200	70	2.13	0.81	26	426	2.10	-	[43]
17	CA060C	1.50	200	200	70	2.13	0.81	26	426	0.81	-	
18	C1	1.50	300	300	160	1.69	0.08	14	587	0.46	2.33	[44]
19	C12	1.50	300	300	75	1.69	0.28	18	384	1.21	8.15	
20	C4	1.50	300	300	75	1.69	0.28	14	587	1.08	5.57	
21	C8	1.50	300	300	75	1.69	0.28	18	384	0.74	2.21	
22	D1	1.00	300	300	50	1.69	0.42	28	398	0.73	3.96	[45]
23	D11	1.50	300	300	150	2.25	0.14	28	398	0.66	1.89	
24	D12	1.50	300	300	150	2.25	0.14	28	398	0.69	1.98	
25	D14	1.50	300	300	50	2.25	0.42	26	398	1.49	17.98	
26	D16	1.00	300	300	50	1.69	0.42	26	398	0.75	8.45	
27	B3	2.00	250	250	60	2.43	0.63	100	344	1.11	-	
28	B4	2.00	250	250	60	2.43	0.52	100	1126	2.34	-	
29	B5	2.00	250	250	30	2.43	1.05	100	774	1.18	-	
30	B6	2.00	250	250	60	2.43	0.52	100	857	1.32	-	
31	B7	2.00	250	250	30	1.81	0.52	100	774	0.54	-	[47]
32	UC15H	2.00	225	225	45	1.86	1.27	118	1424	1.40	-	
33	UC15L	2.00	225	225	45	1.86	1.27	118	1424	2.36	-	
34	UC20H	2.00	225	225	35	1.86	1.63	118	1424	2.30	-	
35	UC20L	2.00	225	225	35	1.86	1.63	118	1424	2.93	-	[48]
36	CUS	1.11	230	410	89	3.01	0.55	35	414	0.69	-	
37	CUW	1.98	410	230	89	3.01	0.15	35	414	1.21	-	
38	UM207	2.00	200	200	100	1.99	0.28	18	324	0.81	-	[49]
39	HC4-8L16-T10-0.2P	2.00	254	254	51	2.46	1.64	86	510	5.84	-	
40	No.1	2.00	300	300	100	2.68	0.19	31	392	0.64	-	[50]
41	No.3	2.00	300	300	200	2.68	0.09	31	392	0.55	8.00	
42	No.4	2.00	300	300	100	2.68	0.19	31	392	0.62	1.95	
43	BE	1.00	175	175	110	2.42	0.29	33	312	0.28	2.01	[51]
44	CE	1.00	175	175	110	2.42	0.29	26	312	0.28	-	
45	LE	1.00	175	175	20	6.94	1.62	42	322	0.77	-	
46	104-08	1.00	160	160	40	2.22	0.61	20	559	0.56	-	[29]
47	204-08	2.00	160	160	40	2.22	0.61	21	559	1.10	-	

Among the candidate variables listed above, only the statistically significant variables used to predict the deformation parameters were selected. To determine the statistically significant variables,

a linear stepwise regression analysis [56] was used. A candidate variable is considered to be statistically significant, when the  $p$ -value is less than 5%. The  $p$ -value is used for measuring the plausibility of a null hypothesis. Typically, in regression analysis, a null hypothesis is rejected if the  $p$ -value is less than 0.05.

As a result of the regression analysis, the obtained equation for parameter  $a$  was written as:

$$a_{fit} = a_{ASCE} + \left( -\frac{1}{47.78} - \frac{1}{57.49} \frac{1}{a_v/h} + \frac{f_{yl}}{1988.07 c_{unit}} \right), \quad (7)$$

where  $c_{unit}$  is 6.89 when using the unit of MPa and 1.00 when using the unit of ksi.

As discussed in the previous section, height-to-depth ratio  $a_v/h$  was found to be a significant predictor variable.

The equation obtained for parameter  $b$  was described as:

$$b_{fit} = b_{ASCE} + \left( \frac{1}{12.56} - \frac{1}{703.39 \rho_l} \right) \geq a_{fit}. \quad (8)$$

In the proposed equations (Equations (7) and (8)), three variables were considered ( $a_v/h$ ,  $\rho_l$ , and  $f_{yl}$ ). It was reported that RC member behavior is affected significantly by  $a_v/h$  [1–6,57]. RC columns with lower  $a_v/h$  are more likely to fail in shear. Past studies [7–9] also reported that the dowel action of longitudinal reinforcements significantly affects the load–deformation responses of stocky structural components; thus,  $\rho_l$  and  $f_{yl}$  selected from the stepwise regression analyses can be physically meaningful variables.

The significant predictor variable for both modeling parameters  $a$  and  $b$  was related to the longitudinal reinforcement, that is, the measured yield strength of a longitudinal reinforcement  $f_{yl}$  and the longitudinal reinforcement ratio  $\rho_l$ . Past literatures [58–60] also revealed that dowel action of longitudinal reinforcements can have significant impact on load–deformation response of relatively stocky structural components.

As discussed in the previous section, due to the scarcity of column specimens tested to the onset of axial failure, Equation (8) was proposed for column specimens experiencing a 75% lateral resistance degradation in Table 2, which corresponded to the 15 RC column specimens.

## 6. Validation of the Proposed Calibration Factor

Figure 4 shows the accuracy of the calculated values of modeling parameters  $a$  and  $b$  with respect to the corresponding measured values. As shown in Figure 4, the calculated values of parameters  $a$  and  $b$  by applying the calibration factor proposed by this study match the corresponding measured values more accurately than those obtained without applying the calibration factor. The errors associated with parameters  $a$  and  $b$  were calculated using Equation (6).

The values of *Error* associated with the calculated values of parameter  $a$  without applying the proposed calibration factor is 87.7%, whereas that by applying the calibration factor is 41.4%. Similar results were obtained for parameter  $b$ .

Envelope curves were plotted for specimens, which were obtained using the ASCE 41-17 equations for parameters  $a$  and  $b$  with and without the proposed calibrating factor applied. Figure 5 show the envelope curves and the measured cyclic curves for the specimens No.4, C1, C8, and N27-C. It was observed that the envelope curves obtained with the proposed calibration factor match the measured cyclic curves more accurately than those obtained without the calibration factor. Similar observations were obtained for the other specimens listed in Table 2, which were not included in this paper due to page limitations.

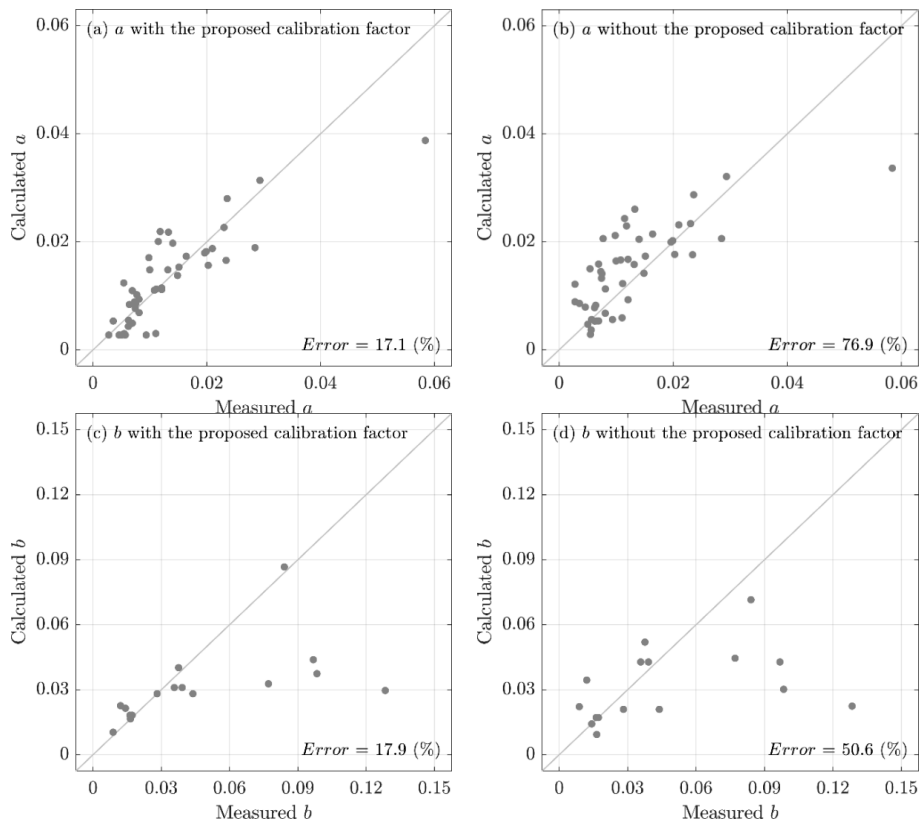


**Figure 4.** Accuracies of the calculated values of modeling parameter  $a$  by applying the proposed calibration factor (a) and without applying the proposed calibration factor (b). Accuracies of the calculated values of modeling parameter  $b$  by applying the proposed calibration factor (c) and without applying the proposed calibration factor (d).

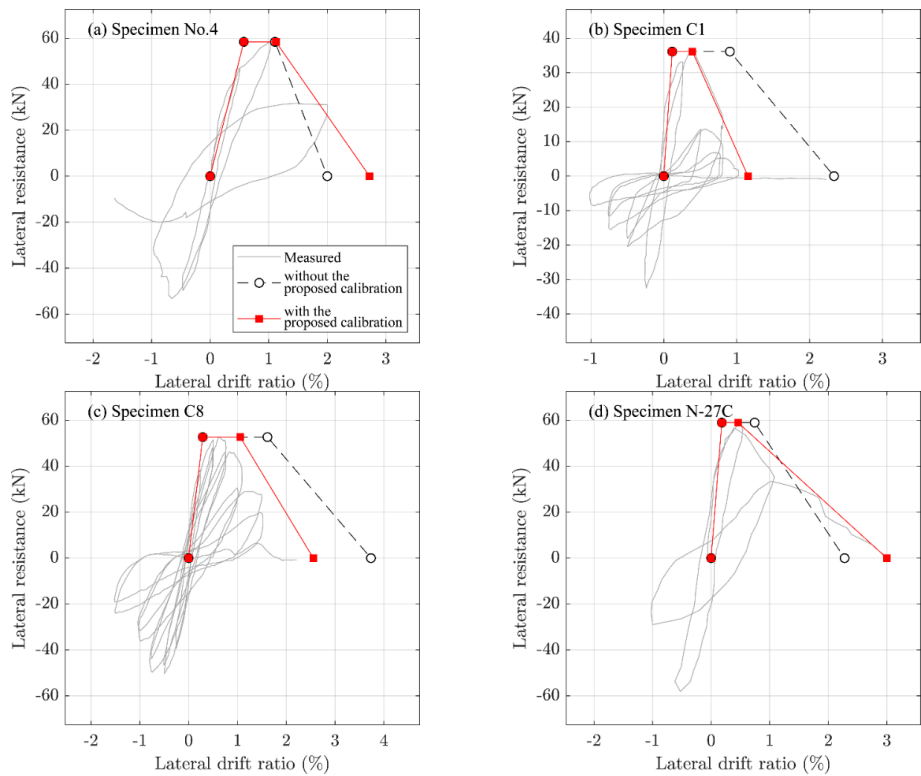


**Figure 5.** Predicted envelope curves and measured cyclic curves.

## 7. Conclusions

In this study, a database of 47 stocky RC columns was used to extract the modeling parameters for constructing column envelope curves. The extracted values were then compared with the modeling parameters values calculated using the ASCE 41-17 equations. The comparison results showed that the error between the measured values and the values calculated with the ASCE 41-17 equations was significant for the columns with height-to-depth ratios ( $a_v/h$ ) less than 2.0. In this study, a calibration factor was proposed for RC columns with  $a_v/h$  less than 2.0 to improve the accuracy of the values of modeling parameters  $a$  and  $b$  calculated from the ASCE 41-17 equations. The following conclusion can be drawn.

1. The ASCE 41-17 equations for deformation modeling parameters produce erroneous predictions for stocky RC columns, because these equations do not consider the effect of  $a_v/h$  of RC columns. The application of the proposed calibration factor significantly improved the accuracy of the calculated values of modeling parameters  $a$  and  $b$  for columns with  $a_v/h$  less than 2.0.
2. After applying the calibration factor to the ASCE 41-17 equations, errors in the calculated values of modeling parameters  $a$  and  $b$  significantly decreased. For parameter  $a$ , the error reduced from 87.7% to 41.4%, and for parameter  $b$ , the error reduced from 71.1% to 42.3%.
3. The envelope curves for the stocky RC columns were accurately constructed using the modeling parameters with the proposed calibration factor, which match the measured cyclic curves.

**Author Contributions:** Conceptualization, S.W.H.; methodology, C.S.L.; investigation, C.S.L., M.A.P.Z., K.L.; writing of the original draft preparation, S.W.H., M.A.P.Z.; writing of review and editing, S.W.H.; visualization, C.S.L.; supervision, S.W.H.; project administration, S.W.H.

**Funding:** This research was funded by the Korea Agency for Infrastructure Technology Advancement (grant number 19CTAP-C152179-01).

**Acknowledgments:** The research was supported by a grant from the Korea Agency for Infrastructure Technology (19CTAP-C152179-01). The valuable comments of four anonymous reviewers are greatly appreciated.

**Conflicts of Interest:** The authors declare no conflicts of interest.

## References

1. Lynn, A.C.; Moehle, J.P.; Mahin, S.A.; Holmes, W.T. Seismic evaluation of existing reinforced concrete building columns. *Earthq. Spectra* **1996**, *12*, 715–739. [[CrossRef](#)]
2. Sezen, H.; Whittaker, A.S.; Elwood, K.J.; Mosalam, K.M. Performance of reinforced concrete buildings during the August 17, 1999 Kocaeli, Turkey earthquake, and seismic design and construction practise in Turkey. *Eng. Struct.* **2003**, *25*, 103–114. [[CrossRef](#)]
3. Humar, J.M.; Lau, D.; Pierre, J.-R. Performance of buildings during the 2001 Bhuj earthquake. *Can. J. Civ. Eng.* **2001**, *28*, 979–991. [[CrossRef](#)]
4. Kam, W.Y.; Pampanin, S.; Dhakal, R.; Gavin, H.P.; Roeder, C. Seismic performance of reinforced concrete buildings in the September 2010 Darfield (Canterbury) earthquake. *Bull. N. Z. Soc. Earthq. Eng.* **2010**, *43*, 340–350. [[CrossRef](#)]
5. Galal, K.; Arafa, A.; Ghobarah, A. Retrofit of RC square short columns. *Eng. Struct.* **2005**, *27*, 801–813. [[CrossRef](#)]
6. Liel, A.B.; Haselton, C.B.; Deierlein, G.G. Seismic collapse safety of reinforced concrete buildings. II: Comparative assessment of nonductile and ductile moment frames. *J. Struct. Eng.* **2011**, *137*, 492–502. [[CrossRef](#)]
7. Lee, C.S.; Han, S.W. Cyclic behaviour of lightly-reinforced concrete columns with short lap splices subjected to unidirectional and bidirectional loadings. *Eng. Struct.* **2019**, *189*, 373–384. [[CrossRef](#)]
8. Harries, K.A.; Ricles, J.M.; Pessiki, S.; Sause, R. Seismic retrofit of lap splices in nonductile columns using CFRP jackets. *ACI Struct. J.* **2006**, *103*, 874–884. [[CrossRef](#)]

9. Melek, M.; Wallace, J. Performance of columns with short lap splices. In Proceedings of the 13th World Conference on Earthquake Engineering, Vancouver, BC, Canada, 1–6 August 2004.
10. Cho, J.-Y.; Pincheira, J.A. Nonlinear modeling of RC columns with short lap splices. In Proceedings of the 13th World Conference on Earthquake Engineering, Vancouver, BC, Canada, 1–6 August 2004.
11. Kim, C.-G.; Park, H.-G.; Eom, T.-S. Seismic performance of reinforced concrete columns with lap splices in plastic hinge region. *ACI Struct. J.* **2018**, *115*, 235–245. [[CrossRef](#)]
12. Sezen, H.; Moehle, J.P. Shear strength model for lightly reinforced concrete columns. *J. Struct. Eng.* **2004**, *130*, 1692–1703. [[CrossRef](#)]
13. Sezen, H.; Moehle, J.R. Seismic tests of concrete columns with light transverse reinforcement. *ACI Struct. J.* **2006**, *103*, 842–849. [[CrossRef](#)]
14. Elwood, K.J.; Moehle, J.P. Drift capacity of reinforced concrete columns with light transverse reinforcement. *Earthq. Spectra* **2005**, *21*, 71–89. [[CrossRef](#)]
15. Elwood, K.J.; Moehle, J.P. Axial capacity model for shear-damaged columns. *ACI Struct. J.* **2005**, *102*, 578–587. [[CrossRef](#)]
16. Baradaran Shoraka, M.; Elwood, K.J. Mechanical model for non ductile reinforced concrete columns. *J. Earthq. Eng.* **2013**, *17*, 937–957. [[CrossRef](#)]
17. Elwood, K.J.; Moehle, J.P. Dynamic collapse analysis for a reinforced concrete frame sustaining shear and axial failures. *Earthq. Eng. Struct. Dyn.* **2008**, *37*, 991–1012. [[CrossRef](#)]
18. Moehle, J.P.; Mahin, S.A. Observations on the behavior of reinforced concrete buildings during earthquakes. *ACI Symp. Publ.* **1991**, *127*, 67–90. [[CrossRef](#)]
19. Haselton, C.B.; Liel, A.B.; Taylor-Lange, S.C.; Deierlein, G.G. Calibration of model to simulate response of reinforced concrete beam-columns to collapse. *ACI Struct. J.* **2016**, *113*, 1141–1152. [[CrossRef](#)]
20. Sezen, H.; Chowdhury, T. Hysteretic model for reinforced concrete columns including the effect of shear and axial load failure. *J. Struct. Eng.* **2009**, *135*, 139–146. [[CrossRef](#)]
21. Ghannoum, W.M.; Moehle, J.P. Rotation-based shear failure model for lightly confined RC columns. *J. Struct. Eng.* **2012**, *138*, 1267–1278. [[CrossRef](#)]
22. Elwood, K.J.; Eberhard, M.O. Effective stiffness of reinforced concrete columns. *ACI Struct. J.* **2009**, *106*, 476–484. [[CrossRef](#)]
23. ASCE 41-17. *Seismic Evaluation and Retrofit of Existing Buildings*; American Society of Civil Engineers: Reston, VA, USA, 2017. [[CrossRef](#)]
24. Ghannoum, W.M.; Matamoros, A.B. Nonlinear modeling parameters and acceptance criteria for concrete columns. *ACI Spec. Publ.* **2014**, *297*, 1–24.
25. ASCE 41-13. *Seismic Evaluation and Retrofit of Existing Buildings*; American Society of Civil Engineers: Reston, VA, USA, 2014. [[CrossRef](#)]
26. Wen, Y.K.; Collins, K.R.; Han, S.W.; Elwood, K.J. Dual-level designs of buildings under seismic loads. *Struct. Saf.* **1996**, *18*, 195–224. [[CrossRef](#)]
27. Lee, L.H.; Lee, H.H.; Han, S.W. Method of selecting design earthquake ground motions for tall buildings. *Struct. Des. Tall Build.* **2000**, *9*, 201–213. [[CrossRef](#)]
28. Elwood, K.J.; Matamoros, A.B.; Wallace, J.W.; Lehman, D.E.; Heintz, J.A.; Mitchell, A.D.; Moore, M.A.; Valley, M.T.; Lowes, L.N.; Comartin, C.D.; et al. Update to ASCE/SEI 41 concrete provisions. *Earthq. Spectra* **2007**, *23*, 493–523. [[CrossRef](#)]
29. Zhou, X.; Satoh, T.; Jiang, W.; Ono, A.; Shimizu, Y. Behavior of reinforced concrete short column under high axial load. *Trans. Jpn. Concr. Inst.* **1987**, *9*, 541–548.
30. Han, S.W.; Lee, C.S.; Shin, M.; Lee, K. Cyclic performance of precast coupling beams with bundled diagonal reinforcement. *Eng. Struct.* **2015**, *93*, 142–151. [[CrossRef](#)]
31. Chen, Z.; Ding, Y.; Shi, Y.; Li, Z. A vertical isolation device with variable stiffness for long-span spatial structures. *Soil Dyn. Earthq. Eng.* **2019**, *123*, 543–558. [[CrossRef](#)]
32. Moretti, M.; Tassios, T.P. Behaviour of short columns subjected to cyclic shear displacements: Experimental results. *Eng. Struct.* **2007**, *29*, 2018–2029. [[CrossRef](#)]
33. FEMA P440A. *Effects of Strength and Stiffness Degradation on Seismic Response*; 440A; Department of Homeland Security: Washington, DC, USA, 2009.
34. Berry, M.P.; Eberhard, M.O. *Performance Models for Flexural Damage in Reinforced Concrete Columns*; Pacific Earthquake Engineering Research Center: Berkeley, CA, USA, 2004.

35. Berry, M.; Parrish, M.; Eberhard, M. *PEER Structural Performance Database User's Manual*; University of California, Berkeley: Berkeley, CA, USA, 2004.
36. Aboutaha, R.S.; Engelhardt, M.D.; Jirsa, J.O.; Kreger, M.E. Rehabilitation of shear critical concrete columns by use of rectangular steel jackets. *ACI Struct. J.* **1999**, *96*, 68–78. [[CrossRef](#)]
37. Amitsu, S.; Shirai, N.; Adachi, H.; Ono, A. Deformation of reinforced concrete column with high or fluctuating axial force. *Trans. Jpn. Concr. Inst.* **1991**, *13*, 355–362.
38. Esaki, F. Reinforcing effect of steel plate hoops on ductility of R/C square columns. In Proceedings of the 11th World Conference on Earthquake Engineering, Acapulco, Mexico, 23–28 June 1996.
39. Iwasaki, T.; Kawasima, K.; Hagiwara, R.; Koyama, T.; Yoshida, T. *Experimental Investigation on Hysteretic Behavior of Reinforced Concrete Bridge Pier Columns*; Public Works Research Institute: Tsukuba, Japan, 1985.
40. Nagasaka, T. Effectiveness of steel fiber as web reinforcement in reinforced concrete columns. *Trans. Jpn. Concr. Inst.* **1982**, *4*, 493–500.
41. Nakamura, T.; Yoshimura, M. Gravity load collapse of reinforced concrete columns with brittle failure modes. *J. Asian Arch. Build. Eng.* **2002**, *1*, 21–27. [[CrossRef](#)]
42. Ohue, M.; Morimoto, H.; Fujii, S.; Morita, S. The behavior of RC short columns failing in splitting bond-shear under dynamic lateral loading. *Trans. Jpn. Concr. Inst.* **1985**, *7*, 293–300.
43. Ono, A.; Shirai, N.; Adachi, H.; Sakamaki, Y. Elasto-plastic behavior of reinforced concrete column with fluctuating axial force. *Trans. Jpn. Concr. Inst.* **1989**, *11*, 239–246.
44. Ousalem, H.; Kabeyasawa, T.; Tasai, A.; Ohsugi, Y. Experimental study on seismic behavior of reinforced concrete columns under constant and variable axial loadings. In Proceedings of the Japan Concrete Institute, Tsukuba, Japan, June 2002.
45. Ousalem, H.; Kabeyasawa, T.; Tasai, A. Effect of hysteretic reversals on lateral and axial capacities of reinforced concrete columns. In Proceedings of the Fifth U.S.-Japan Workshop on Performance-Based Earthquake Engineering Methodology for Reinforced Concrete Structures, Hakone, Japan, 10–11 September 2003.
46. Sakai, Y.; Hibi, J.; Otani, S.; Aoyama, H. Experimental study on flexural behavior of reinforced concrete columns using high-strength concrete. *Trans. Jpn. Concr. Inst.* **1990**, *12*, 323–330.
47. Sugano, S. Seismic behavior of reinforced concrete columns which used ultra-high-strength concrete. In Proceedings of the 11th World Conference on Earthquake Engineering, Acapulco, Mexico, 23–28 June 1996.
48. Umehara, H.; Jirsa, J.O. *Shear Strength and Deterioration of Short Reinforced Concrete Columns Under Cyclic Deformations*; PMFSEL Report No. 82-3; University of Texas at Austin: Austin, TX, USA, 1982.
49. Xiao, Y.; Martirosyan, A. Seismic performance of high-strength concrete columns. *J. Struct. Eng.* **1998**, *124*, 241–251. [[CrossRef](#)]
50. Takaine, Y.; Yoshimura, M.; Nakamura, T. Collapse drift of reinforced concrete columns. *J. Struct. Constr. Eng. (Trans. AIJ)* **2003**, *68*, 153–160. [[CrossRef](#)]
51. Yoshimura, K.; Kikcuri, K.; Kuroki, M. Seismic shear strengthening method for existing R/C short columns. *ACI Spec. Publ.* **1991**, *128*, 1065–1080. [[CrossRef](#)]
52. LeBorgne, M.R.; Ghannoum, W.M. Calibrated analytical element for lateral-strength degradation of reinforced concrete columns. *Eng. Struct.* **2014**, *81*, 35–48. [[CrossRef](#)]
53. Han, S.W.; Koh, H.; Lee, C.S. Accurate and efficient simulation of cyclic behavior of diagonally reinforced concrete coupling beams. *Earthq. Spectra* **2019**, *35*, 361–381. [[CrossRef](#)]
54. Lee, C.S.; Han, S.W. Computationally effective and accurate simulation of cyclic behaviour of old reinforced concrete columns. *Eng. Struct.* **2018**, *173*, 892–907. [[CrossRef](#)]
55. Elwood, K.J. Modelling failures in existing reinforced concrete columns. *Can. J. Civ. Eng.* **2004**, *31*, 846–859. [[CrossRef](#)]
56. Chatterjee, S.; Hadi, A.S. *Regression Analysis by Example*, 4th ed.; Wiley Series in Probability and Statistics; Wiley: Hoboken, NJ, USA, 2006. [[CrossRef](#)]
57. Shin, M.; Gwon, S.-W.; Lee, K.; Han, S.W.; Jo, Y.W. Effectiveness of high performance fiber-reinforced cement composites in slender coupling beams. *Constr. Build. Mater.* **2014**, *68*, 476–490. [[CrossRef](#)]
58. Barney, G.B.; Shiu, K.N.; Rabbat, B.G.; Fiorato, A.E.; Russell, H.G.; Corley, W.G. *Behavior of Coupling Beams Under Load Reversals (RD068.01B)*; Portland Cement Association: Skokie, IL, USA, 1980.

59. Breña, S.F.; Ihtiyar, O. Performance of conventionally reinforced coupling beams subjected to cyclic loading. *J. Struct. Eng.* **2011**, *137*, 665–676. [[CrossRef](#)]
60. Ding, R.; Tao, M.-X.; Nie, J.-G.; Mo, Y.L. Shear deformation and sliding-based fiber beam-column model for seismic analysis of reinforced concrete coupling beams. *J. Struct. Eng.* **2016**, *142*, 04016032. [[CrossRef](#)]



© 2019 by the authors. Licensee MDPI, Basel, Switzerland. This article is an open access article distributed under the terms and conditions of the Creative Commons Attribution (CC BY) license (<http://creativecommons.org/licenses/by/4.0/>).